JTTEE5 15:570-575
DOI: 10.1361/105996306X146703
1059-9630/$19.00 © ASM International

Peer Reviewed

# Effect of Particle Impact on Residual Stress Development in HVOF Sprayed Coatings

*P. Bansal, P.H. Shipway, and S.B. Leen*

*(Submitted February 27, 2006; in revised form June 27, 2006)*

**The application of thick high-velocity oxyfuel (HVOF) coatings on metallic parts has been widely accepted as a solution to improve their wear properties. The adherence of these coatings to the substrate is strongly influenced by the residual stresses generated during the coating deposition process. In an HVOF spraying process, due to the relatively low processing temperature, significant peening stresses are generated during impact of molten and semimolten particles on the substrate. At present, finite-element (FE) models of residual stress generation for the HVOF process are not available due to the increased complexities in modeling the stresses generated due to the particle impact. In this work, an explicit FE analysis is carried out to study the effect of molten particle impingement using deposition of an HVOF sprayed copper coating on a copper substrate as an example system. The results from the analysis are subsequently used in a thermomechanical FE model to allow the development of the residual stresses in these coatings to be modeled.**

**Keywords** copper, finite element, high-velocity oxyfuel, particle impact, residual stress

## 1. Introduction

Coating deposition using a thermal spray process is generally associated with the development of residual stresses in the coating. These stresses, which vary in nature and magnitude depending on the process used, have a pronounced effect on the mechanical behavior of the coating. Residual stresses have been reported to influence the wear and fatigue resistance of the coatings (Ref 1-3) and their resistance to cracking (Ref 4-6).

The significant effect of residual stresses on the performance of a coated component indicates the need to study the development of these stresses. Residual stress generation in thermally sprayed coatings has been well researched by various workers. Tsui et al. (Ref 7) suggested that the residual stresses are generated from two main sources during thermal spraying. Sprayed molten particles impinging on the substrate form flat splats and quench to the substrate temperature within a few milliseconds. The underlying substrate constrains the thermal contraction of the splats, resulting in tensile stresses (quenching stresses) in the splats. Later on, further cooling of the sprayed coating and the substrate to the ambient temperature leads to thermal stresses in the coated specimen. This mechanism of residual stress generation is applicable for processes where fully molten particles are sprayed with low velocity. Plasma spraying is one such thermal spray technique. On the other hand, processes such as the high-velocity oxyfuel (HVOF) process use low spray temperatures and high particle velocities. In such processes, the kinetic energy of the molten and partially molten particles leads to significant peening of the substrate, thereby influencing the final state of residual stresses (Ref 8). Pina et al. (Ref 9) proposed that during the HVOF spray process, residual stresses are generated in two stages. In the first stage, the sprayed particles impinging on the substrate induce mechanical stresses in the substrate. During this stage, quenching stresses are also generated in the particle and the substrate as the deposited particle cools down to the underlying substrate temperature. Later on, in the second stage, further cooling of the sprayed coating and the substrate to the ambient temperature leads to the differential thermal contraction, which in turn results in thermal stresses in the substrate and the coating. Hence, residual stress generation in thermally sprayed coatings can be broadly attributed to:

- Mechanical stresses due to the impinging molten and partially molten droplets on the substrate
- Phase transitions in the coating material during the deposition process
- Quenching stresses due to splat solidification
- Secondary cooling stresses due to the differential cooling of the substrate and the coating to the room temperature

The final residual stress in the coating is obtained by superimposing the individual stresses generated due to these factors. In this work, finite-element (FE) tools are used to study the residual stress generation during deposition of a copper coating on copper substrate by HVOF spraying of molten particles. This system was chosen for the model since copper has exceptionally well-attested material property data at high strain rates (Johnson-Cook data) (Ref 10). Finite-element-predicted trends are then compared with the results available in the literature on similar coating systems.

This article was originally published in *Building on 100 Years of Success, Proceedings of the 2006 International Thermal Spray Conference* (Seattle, WA), May 15-18, 2006, B.R. Marple, M.M. Hyland, Y.-Ch. Lau, R.S. Lima, and J. Voyer, Ed., ASM International, Materials Park, OH, 2006.

**P. Bansal, P.H. Shipway,** and **S.B. Leen,** School of Mechanical, Materials and Manufacturing Engineering, University of Nottingham, University Park, Nottingham NG7 2RD, U.K. Contact e-mail: emxpb@nottingham.ac.uk.

**Table 1 Spray parameters and powder properties**

| | |
|---|---|
| Powder feed rate, g/min | 75 |
| Density of Cu, kg/m$^3$ | 8960 |
| Diameter of deposition zone, mm | 28.6 |
| Average particle size, μm | 50 |
| Total splat area/deposition zone area | $2.4 \times 10^{-4}$ |

Source: Ref 15, 16

## 2. Methodology

### 2.1 Thermally Sprayed Coating Deposition Process

In a thermal spray process, powder particles are fed into a stream of a hot carrier gas and propelled toward a substrate at a high velocity. Upon impact, these particles undergo severe deformation within a very short interval of time. Flattening of these particles leads to the formation of splats, which are considered to be the building blocks of the sprayed coating (Ref 11-14). In the current study, a deposition process using a JP-5000 HVOF system is considered. The JP-5000 spray system delivers a spray stream of approximately 29 mm width and a well-defined HVOF particle deposition zone with relatively constant particle temperature and velocity across it (Ref 15). Interaction between the particle and the gas during the HVOF spray process has been extensively researched by various workers (Ref 12, 14). Using their multiscale model of an industrial HVOF thermal spray process, Li et al. (Ref 14) showed that during the deposition process, individual powder particles in the gas stream can be considered isolated from each other. They therefore, postulated that no powder coagulation takes place during the flight, and hence the powder size distribution remains unchanged during the spray process. On deposition, particles will deform and cool; however, for a wide range of commonly used deposition conditions, it can be shown that an individual particle will have cooled to a temperature less than a third of its absolute melting temperature (~0.33 $T_m$) before another particle is likely to interact with it. For example, using the deposition data for HVOF spraying of copper shown in Table 1, it can be shown that the incident particle flux is around $3.3 \times 10^9$ particles m$^{-2}$ s$^{-1}$. Given that it can be estimated by FE modeling that an individual particle will cool to 0.33 $T_m$ in around 0.6 ms, then it can be shown that within this timeframe, the particle coverage (assuming a splat diameter of 4.5 times the original particle diameter of 50 μm, Ref 17) is only around 9% of the total area. If it is assumed that the particles deposit in the form of a hexagonal lattice, it can be shown that, in this case, this represents splats of 250 μm diameter with a center-center distance of 1400 μm. As such, it can be shown that the assumption of the particles being noninteracting during deposition is reasonable and indicates that a thermally sprayed coating is formed by the consecutive flattening and solidification of individual splats.

### 2.2 FE Modeling of the Residual Stress Generation

Coating deposition using the HVOF spray method is a dynamic process involving rapid deformation and solidification of the sprayed particles followed by cooling down of the coated specimen to the ambient temperature. In the present work, two different FE analyses were performed. Residual stresses generated during the impact process were introduced in the final stress analysis. Figure 1 illustrates the methodology used to determine the final residual stress distribution.

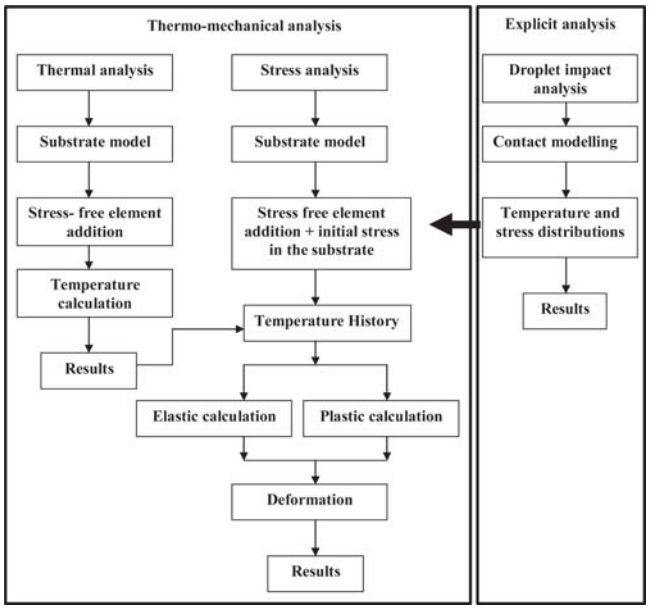


**Fig. 1** Flowchart of the methodology used to determine the final residual stress distribution

### 2.3 FE Model of the Particle Impact

A three-dimensional model of a 50 μm diameter copper particle impacting on a copper substrate ($0.3 \times 0.32 \times 0.3$ mm$^3$) was generated using ABAQUS CAE version 6.5.1 (ABAQUS, Inc., Providence, RI). A dynamic, explicit temperature-displacement coupled analysis was carried out to study the high strain rate impact process using the ABAQUS/Explicit (ABAQUS, Inc., Providence, RI). Heat transfer mechanisms included in the model are:

- Conduction in substrate
- Conduction in particle/ splat
- Conduction and radiation across the particle-substrate interface

Four-node tetrahedron elements were used for the particle. Eight-node trilinear elements with reduced integration and hourglass control were used for the substrate. Figure 2 illustrates the FE model of the impacting particle on the substrate.

In an explicit analysis, the stable time increment is given as (Ref 18):

$$\Delta t_{\text{stable}} = \frac{L_e}{c_d} \quad \text{(Eq 1)}$$

where, $L_e$ is the smallest element dimension and $c_d$ is the wave speed of the material. The wave speed of a material with an elastic modulus $E$ and density ρ is given by:

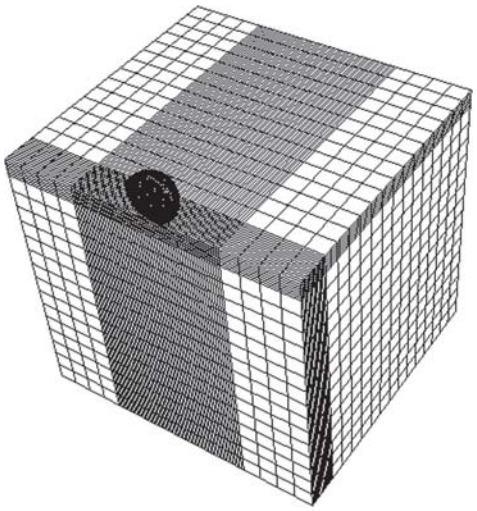

**Fig. 2** FE model of copper particle impact on a copper substrate

$$c_d = \sqrt{\frac{E}{\rho}} \quad \text{(Eq 2)}$$

The requirement for a fine mesh with small elements to capture the detailed stress distributions therefore leads to very short maximum allowable time increments that in turn result in a computationally time-intensive analysis. To optimize the computational efficiency of the impact model, smaller elements were used only along the particle/substrate interface. A mesh convergence study was carried out using the total kinetic energy of the system as the convergence criteria. The final (converged) mesh adopted here has 59,229 elements and 53,096 nodes, which is accurate to within 0.5% of the numerically obtained kinetic energy of the particle.

The FE analysis assumes that after the first contact during impact, the particle remains attached to the substrate. This behavior was modeled by assigning a contact with a no separation criteria between the contacting nodes of the impinging particle and the underlying substrate. The material properties for copper used in the FE model are listed in Table 2. The plastic response of the sprayed copper particles during the deposition process was defined using the Johnson-Cook plasticity model, which is suited to model the high-strain rate deformation of metals. Using the Johnson-Cook model, the yield stress is expressed as (Ref 18):

$$\overline{\sigma} = [A + B(\bar{\varepsilon}^{pl})^n]\left[1 + C \ln\left(\frac{\dot{\bar{\varepsilon}}^{pl}}{\dot{\varepsilon}_0}\right)\right](1 - \hat{\theta}^m) \quad \text{(Eq 3)}$$

where $\bar{\varepsilon}^{pl}$ is the equivalent plastic strain, $\dot{\bar{\varepsilon}}^{pl}$ is the equivalent plastic strain rate, $A$, $B$, C, $m$, $n$, $\dot{\varepsilon}_0$ are material parameters measured at or below the transition temperature, and $\hat{\theta}$ is a nondimensional temperature, defined as:

$$\hat{\theta} = \begin{cases} 0 & \text{For } \theta < \theta_{transition} \\ \dfrac{(\theta - \theta_{transition})}{(\theta_{melt} - \theta_{transition})} & \text{For } \theta_{transition} \geq \theta \geq \theta_{melt} \\ 1 & \text{For } \theta > \theta_{melt} \end{cases} \quad \text{(Eq 4)}$$

**Table 2 Thermomechanical properties of copper**

| | |
|---|---|
| Elastic modulus, GPa | 124 |
| Yield stress, MPa | |
| at 298 K | 104 |
| at 500 K | 87 |
| at 730 K | 65 |
| Density, kg/m$^3$ | 8960 |
| Specific heat capacity J/kg · K | 383 |
| Thermal conductivity, W/K · m$^2$ | |
| at 300 K | 398 |
| at 800 K | 371 |
| at 1356 K | 33 |
| Coefficient of thermal expansion, K$^{-1}$ | $5 \times 10^{-5}$ |
| Latent heat of fusion, J/kg | 205 |
| Emissivity | 0.1 |
| Gap conduction coefficient, W/K · m$^2$ | 330 |

Source: Ref 10, 19

where $\theta_{transition}$ is the temperature above which thermal softening is assumed to occur. The Johnson-Cook parameters used in the FE model for copper are listed in Table 3. In the model, HVOF spray conditions were characterized by the particle velocity and the particle temperature. These parameters were considered as the key variables in the FE model. Two different analyses were performed with the particle temperature of 1400 K (Ref 20) and velocities of 400 and 500 m/s.

### 2.4 Thermomechanical FE Model

Explicit modeling of the single-particle impact requires significant computation time. Similar analysis for a small region formed by multiple particles is highly time intensive. To overcome this problem, a two-dimensional, FE model of a progressively deposited coating on a thick substrate was developed. The residual stress generation during the coating deposition was then studied using a nonlinear, sequentially coupled, thermomechanical FE analysis performed in two stages. In the first stage, a heat transfer analysis was conducted to obtain the thermal history of the specimen. The time-dependent temperature distribution together with the impact stress profile from the explicit model was subsequently used in a stress analysis to evaluate the final residual stress distribution. The thermomechanical properties of copper used in the model are listed in Table 2.

Explicit analysis showed that upon impact, a 50 μm diameter molten particle changes into a disk of approximately 13 μm thickness and 130 μm in diameter. In the thermomechanical analysis, coating growth was modeled by adding a series of ten 13 μm thick layers onto the substrate ($1.3 \times 1.0$ mm$^2$). The width of each layer is taken to be that of ten particles that are assumed to be bonded together. Figure 3 shows the FE model with all layers included. Heat transfer analysis was carried out using the four-node linear diffusive heat transfer elements. The stress analysis used four-node bilinear, reduced-integration plain strain elements with hourglass control. Temperature dependency of the conductivity is modeled. The thermal conductivity of the coating elements was defined using a field variable. Thus, initially all the coating elements were assigned the conductivity of air, and during the spray process to model the deposition of copper particles the conductivity of the added elements was changed to that of copper. Coating growth was then simulated by

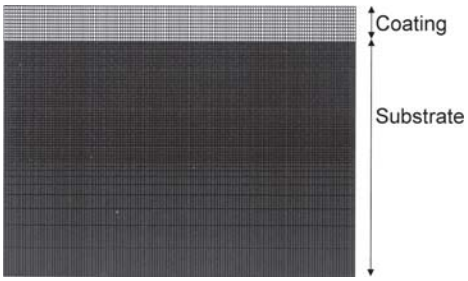


**Fig. 3** Two-dimensional FE model for thermomechanical analysis

**Table 3 Johnson-Cook parameters for copper**

| | |
|---|---|
| $A$, MPa | 90 |
| $B$, MPa | 292 |
| $n$ | 0.31 |
| $C$ | 0.025 |
| $m$ | 1.09 |
| Transition temperature ($\theta_{transition}$), K | 298 |
| Reference strain ($\dot{\varepsilon}_0$), $s^{-1}$ | 1 |

Source: Ref 10

the successive addition of such layers. A 10 s delay was permitted between the arrivals of the consecutive layers to account for the gun movement during the spraying process. Heat transfer between the HVOF jet and the coating was defined as the surface heat flux of 1 MW/m$^2$ in the respective coating top layers (Ref 21). Cooling of the coated specimen to the ambient temperature by natural convection between the coating and the surrounding was modeled. An iterative procedure was used to repeatedly impose the residual stress profile obtained from the explicit analysis for each layer loaded. Similarly, the temperature distribution from the explicit analysis was imposed for each layer added.

## 3. Results and Discussion

### 3.1 Particle Impact Process

Figure 4 illustrates the FE predicted deformation of the particle during impact along with the predicted temperature distribution across the coated substrate and the peening stresses ($\sigma_{xx}$) induced in the substrate due to impact. Note that the $x$-direction is parallel to the free surface. Particle thickness decreases rapidly in the initial stage of impact (Fig. 4a). When sprayed at 400 m/s, the thickness of the particle attains a steady value of ~13 μm. No significant change is observed in the particle thickness after 400 ns after first contact. Increasing the spray velocity to 500 m/s increases the rate of deformation in the early stages of impact. However, the deformation rate gradually decreases and the particle attains a final thickness of ~11 μm. Figure 4(b) illustrates the predicted final temperature distribution across the particle and the substrate thickness. At the end of 400 ns, the coated specimen with the particle sprayed at 500 m/s exhibits a more gradual temperature distribution, although the depth of the affected region in the substrate remains approximately the same for both cases.

A comparison of the rate of temperature change in a node located at the top of the particle is illustrated in Fig. 5. The temperature starts to drop once the particle attains a steady final thickness. This indicates that solidification of the particle begins after completion of the flattening process. Fan et al. studied stress generation during impact of a molten nickel particle onto a flat substrate (Ref 22). They reported that the spreading or flattening time of the droplets was of the order of less than a microsecond, significantly shorter than the estimated solidification time.

During the deposition process, the particle sprayed at 500 m/s attains a final thickness comparable to the particle sprayed at 400 m/s. This can be explained in terms of the two competing mechanisms, namely strain hardening and thermal softening of the particles upon impact. The particle sprayed at 500 m/s exhibits a faster temperature drop, which leads to a reduced degree of thermal softening. Moreover, high-spray velocity also results in a higher strain rate, which leads to significant hardening of the particle. Figure 4(c) illustrates the final $\sigma_{xx}$ distribution through the substrate thickness directly under the point of impact. As expected, particles sprayed at 500 m/s generate significant compressive peening stresses in the substrate. Moreover, these compressive stresses extend to a greater depth into the substrate.

### 3.2 Thermomechanical Analysis

The stress and temperature distributions (Fig. 4b and c) predicted by the explicit analysis of the impact process were introduced in the thermomechanical model. Figure 6 shows the $\sigma_{xx}$ profile through the substrate thickness after an equilibrium step in the thermomechanical analysis.

Close agreement between the target stress profile and the equilibrium distribution illustrates a satisfactory introduction of the peening stresses in the thermomechanical model. The final residual stress distributions predicted by the FE thermomechanical analysis are shown in Fig. 7. Figure 7 shows that larger compressive stresses develop in the deposited coating when the particles are sprayed with a higher velocity. The compressive region, created by the peening action of the sprayed particles, is predicted to extend into the substrate to a few micrometers in depth. Coatings sprayed using a lower spray velocity exhibit tensile stresses on the surface. These tensile stresses are predicted to change through the coating thickness to the high compressive stresses. Similar effects have been achieved for HVOF sprayed coatings by McGrann et al. (Ref 2). However, for proprietary reasons, the values of the spray parameters used were not disclosed.

In the present model, the impinging particle arrives at the substrate in the molten state. In the case of its temperature being greater than its melting point, the Johnson-Cook model of material plasticity assumes the material to have a flow stress of zero. The deformed shape of the molten particle upon impact is thence controlled by the cooling and resolidification of the particle. The predicted (final) deformed shape following impact with the present model is found to be consistent with experimental observations (Ref 16). This approach works well for the present copper system due to the high thermal conductivity of copper leading to resolidification within the time frame of the deformation. However, use of the Johnson-Cook model for materials with low thermal conductivities would lead to nonrealistic deformed shapes due to the particle remaining above its melt-

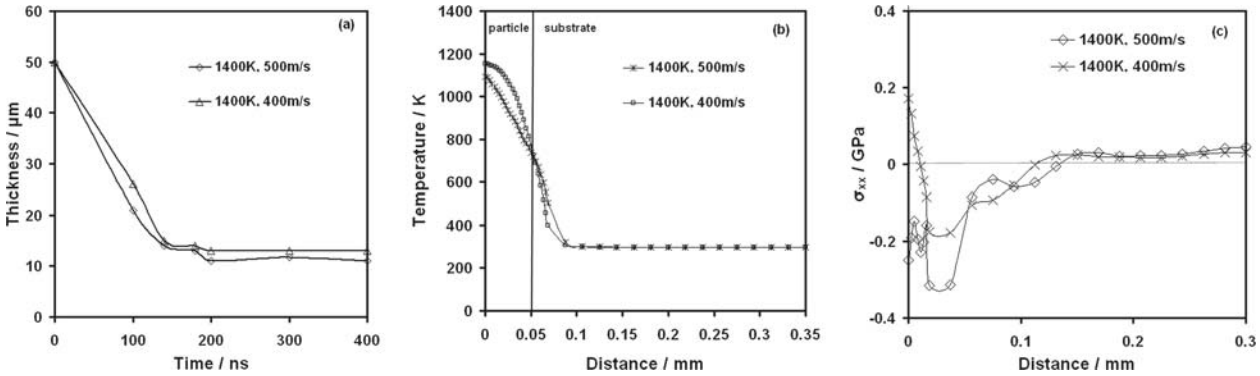


**Fig. 4** FE predicted (a) change in the particle thickness, (b) temperature distribution across the particle and the substrate, and (c) final $\sigma_{xx}$ stress distribution through the substrate thickness, after 400 ns of impact

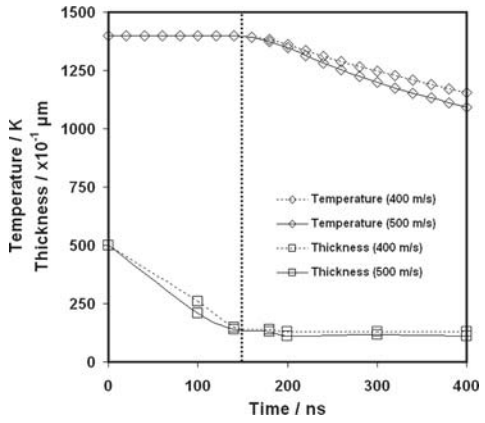


**Fig. 5** Predicted temperature change in the node at the top of the particle and predicted thickness variation of the particle

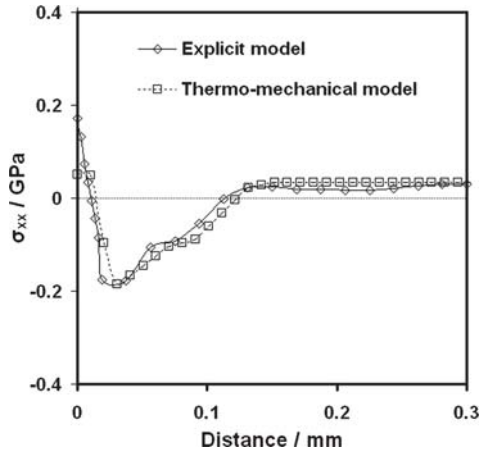


**Fig. 6** Predicted $\sigma_{xx}$ stress profile through the substrate thickness for the particle velocity of 400 m/s

ing temperature throughout the deformation period. In such cases, an alternative material model, for example, the Equation of State model (Ref 23), which uses viscosity to predict splat deformation, is required.

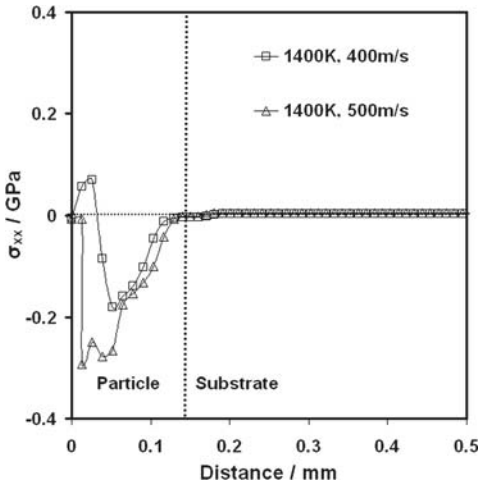


**Fig. 7** Final $\sigma_{xx}$ stress profile through the particle and the substrate thickness for different particle velocities

Present work is limited to the study of the effect of the impingement of a fully molten particle. It is proposed to extend the model to include semimolten particle impingement, which is significantly more complex and would involve a scheme to assign different material properties to different regions of the particle.

## 4. Conclusions

The coating deposition process can be effectively simulated using an explicit FE model. The model predicts similar distributions of the final residual stress to those reported in literature. It also highlights the significant effect of the peening process on the final residual stress state of the component. The development of such a model provides a better understanding of the effect of the processing parameters on the coating properties (residual stresses) and can thus assist in designing coatings with improved performance. Detailed experimental validation is proposed to verify the model.

### References

1. T.W. Clyne, Residual Stresses in Thick and Thin Surface Coating, *Encyclopaedia of Materials: Science and Technology,* Elsevier, 2001

2. R.T.R. McGrann, D.J. Greving, J.R. Shadley, E.F. Rybicki, B.E. Bodger, and D.A. Somerville, The Effect of Residual Stress in HVOF Tungsten Carbide Coatings on the Fatigue Life in Bending of Thermal Spray Coated Aluminium, *J. Therm. Spray Technol,* 1998, **7**(4), p 546-552
3. P.J. Withers and H.K.D. Bhadeshia, Residual Stress Part 1-Measurement techniques, *Mater. Sci. Technol.,* 2001, **17,** p 355-365
4. S. Bouaricha, J.-G. Legoux, and P. Marcoux, Bending Behaviour of HVOF Produced WC-17Co Coatings: Investigated by Acoustic Emission, *J. Therm. Spray Technol,* 2004, **13**(3), p 405-414
5. P. Bansal, P.H. Shipway, and S.B. Leen, Finite Element Modelling of the Fracture Behaviour of Brittle Coatings, *Surf. Coat. Technol,* 2006, **200,** p 5318-5327
6. M. Buchmann, R. Gadow, and J. Tabellion, Experimental and Numerical Residual Stress Analysis of Layer Coated Composites, *Mater. Sci. Eng.,* 2000, **A288,** p 154-159
7. Y.C. Tsui and T.W. Clyne, An Analytical Model for Predicting Residual Stresses in Progressively Deposited Coatings, *Thin Solid Films,* 1997, **306,** p 23-33
8. M. Wenzelburger, Modelling of Thermally Sprayed Coatings on Light Metal Substrates:—Layer Growth and Residual Stress Formation, *Surf. Coat. Technol,* 2004, **180-181,** p 429-435
9. J. Pina, A. Dias, and J.L. Lebrun, Study by X-ray Diffraction and Mechanical Analysis of the Residual Stress Generation During Thermal Spraying, *Mater. Sci. Eng.,* 2003, **A347,** p 21-31
10. G.R. Johnson and W.H. Cook, A Constitutive Model and Data for Metals Subjected to Large Strains, High Strain Rates and High Temperatures, *Proc. Seventh Int. Symp. on Ballistics,* The Netherlands, 1983, p 541-547
11. M.P. Planche, B. Normand, H. Liao, G. Rannou, and C. Coddet, Influence of HVOF Spraying Parameters on In-Flight Characteristics of Inconel 718 Particles and Correlation with the Electrochemical Behaviour of the Coating, *Surf. Coat. Technol,* 2002, **157,** p 247-256
12. T.C. Hanson, C.M. Hackett, and G.S. Settles, Independent Control of HVOF Particles Velocity and Temperature, *J. Therm. Spray Technol,* 2002, **11**(1), p 75-85
13. S.D. Aziz and S. Chandra, Impact, Recoil and Splashing of Molten Metal Droplets, *Int. J. Heat Mass Trans,* 2000, **43,** p 2842-2857
14. M. Li and P.D. Christofides, Multi-Scale Modeling and Analysis of an Industrial HVOF Thermal Spray Process, *Chem. Eng. Sci.,* 2005, **60,** p 3649-3669
15. R.J. Thorpe, L. McGregor, and D. Wang, The JP-5000 HP/HVOF- The Next Generation HVOF, *Proc. Int. Therm. Spray Conf.* (Essen, Germany), DVS/IIW/ASM-TSS, 2002, p 125-135
16. J. Kawakita, K. Isoyama, S. Kuroda, and H. Yumoto, Effects of Deformability of HVOF Sprayed Copper Particles on the Density of Resultant Coatings, *Surf. Coat. Technol,* 2006, April 10, **200**(14-15), p 4414-4423
17. C. Li, H. Liao, P. Gougeon, G. Montavon, and C. Codet, Experimental Determination of The Relationship Between Flattening Degree and Reynolds Number for Spray Molten Droplets, *Surf. Coat. Technol,* 2005, **191,** p 375-383
18. Abaqus/ Explicit User's Manual, Version 6.5-1, H.K.S. Inc.
19. E.G. West, *Copper and its Alloys,* Ellis Horwood Ltd., 1982
20. D.-Y. Ju, V. Ji, and H. Gassot, Computer Predictions Of Thermo-Mechanical Behaviour and Residual Stresses In Spray Coating Process, *J. Phys. IV,* 2004, **120,** p 381-388
21. R. Bolot, C. Verdy, C. Coddet, D. Cornu, and M. Choulant, Analysis of Thermal Fluxes Transferred by an Impinging HVOF Jet, *Proc. Int. Therm. Spray Conf.* (Basel, Switzerland), May 2-4, 2005, E. Lugscheider, Ed., DVS/IIW/ASM-TSS, 2005
22. Q. Fan, L. Wang, F. Wang, and Q. Wang, Modelling of Temperature and Residual Stress Fields Resulting From Impacting Process of a Molten Ni Particle Onto a Flat Substrate, *Proc. Int. Therm. Spray Conf.* (Basel, Switzerland), May 2-4, 2005, E. Lugscheider, Ed., DVS/IIW/ASM-TSS, 2005
23. H. Assadi, F. Gartner, T. Stoltenhoff, and H. Kreye, Bonding Mechanism in Cold Gas Spraying, *Acta Mater.,* 2003, **51,** p 4379-4394